Asian Journal of Chemistry; Vol. 34, No. 12 (2022), 3279-3285

ASIAN JOURNAL OF CHEMISTRY

https://doi.org/10.14233/ajchem.2022.24045

Effect of Photodegradation on Ternary $FeNiS_2$ Thin Film with Complexing Agents EDTA and Leishman Stain

G.D. Gayathri and R. Thiruneelakandan*

Department of Chemistry, University College of Engineering, BIT Campus, Anna University, Tiruchirappalli-620024, India

*Corresponding author: E-mail: rtkchemaut@gmail.com

Received: 29 September 2022; *Accepted*: 16 October 2022; *Published online*: 25 November 2022; AJC-21057

The aim of this study is to analyze the photocatalytic dye degradation efficiency of $FeNiS_2$ with EDTA and Leishman stain thin films prepared using a sol-gel technique. The results of surface morphology and elemental composition, optical characterization of these films obtained using various characterization techniques such as SEM, EDX, UV-VIS spectroscopy. The photocatalytic studies show that the addition of EDTA and Leishman extraordinarily enhances the photocatalytic efficiency of $FeNiS_2$. The $FeNiS_2$ with EDTA, $FeNiS_2$ with Leishman stain thin films causes 92%, 90% and 89% decomposition of methylene blue, malachite green and crystal violet dye molecules, respectively.

Keywords: Iron nickel sulphide, EDTA, EDX, Band gap, Methylene blue.

INTRODUCTION

The majority of current research has focused on thin films with a variety of uses, including photocatalysis, photovoltaics, solar cells and superconducting resources with potential growth [1]. The use of thin films as solar energy transducers is very common [2]. These transducers typically acquire total energy in a linear relationship with surface area. Therefore, in order to collect a lot of energy, solar energy devices may have a big surface area [3]. In this context, numerous binary and ternary II-VI semiconductor resource properties have been studied, and their applications in a number of devices have been established [4-7]. The production of thin films, which are plentiful, inexpensive and non-toxic with a wide range of uses, makes considerable use of substrates and reagent materials. To produce an incredibly thin and uniform film coating, the thin film production and synthesis should be carried out with care.

Studies on ternary chalcogenide materials are attracting considerable interest and is expanding fast [8]. These include uses for nuclear power, industry, medicine and thermoelectricity [9,10]. Many workers reported ternary thin films with a variety of uses, including CuNiS [11], $CuSbS_2$ [12] and Cu_2SnS_3 [13]. Ternary compounds have been researched for use as effective solar energy conversion materials [14,15]. Ternary chalcogenides have undergone much development and characterisation in recent years [16]. Some ternary compounds have been developed for window layer solar cells and optoelectronic devices [17]. The techniques used for the deposition of thin films include chemical bath deposition, molecular beam deposition, spray pyrolysis, flash evaporation and chemical vapour deposition [18].

The chemical bath deposition is one of these technologies that is affordable, practicable and offers a great area for deposition. $CuFeS_2$ and $FeZnS_2$ ternary thin films have recently been the subject of reports on the synthesis and effects of complexing agents [19,20]. It is reported that $FeNiS_2$ is the best alternative to TiO_2 due to its high reactivity, non-toxic nature, low cost and also it act as best photocatalyst. Sindhuja *et al.* [21] reported that $FeNiS_2$ thin films deposited using sol-gel method and the photodegradation activity of the prepared samples are tested against three different dyes like methylene blue, malachite green, crystal violet, respectively. The chemical bath deposition method was used to deposit copper iron sulphide ($FeCuS_2$) thin films utilizing ferrous and copper sulphates as cationic sources and sodium sulphide as an anionic source with complexing agents, EDTA and Leishman stain. As the complexing agents varied, the absorption edge changed toward a lower wavelength and 3.57-3.85 eV was found to be the band gap value [19].

This is an open access journal, and articles are distributed under the terms of the Attribution 4.0 International (CC BY 4.0) License. This license lets others distribute, remix, tweak, and build upon your work, even commercially, as long as they credit the author for the original creation. You must give appropriate credit, provide a link to the license, and indicate if changes were made.

Leishman stain and EDTA both function as complexing agents and are anticipated to be crucial in the development of $FeZnS_2$ thin films. $FeZnS_2$ thin films displayed good optical characteristics and high visible absorption and the band gap was found to in between 2.37 to 2.77 eV [20].

EXPERIMENTAL

Synthesis: In this work, $FeNiS_2$ doped EDTA and $FeNiS_2$ doped Leishman stain films were developed by the sol-gel method as per reported method [21]. The origin solution was processed from ferrous sulphate, nickel nitrate, sodium sulphide and distilled water. A EDTA solution (1 mL) was added to a solution of molar ratio of $FeSO_4{\cdot}7H_2O$:$NiNO_3$:$Na_2S{\cdot}$ $9H_2O$ (0.08:0.08:0.04) dissolved in distilled water and blend for 1 h at room temperature to yield a clear and consistent sol ready for coating. A soda lime glass substrate of 75 mm × 25 mm was pre-cleaned by methanol and ultrasonically handled with acetone. The sol solution was discarded on to the substrate which was rotated at 4000 rpm for 30 s. After degradation by spin coating, the films were dried at 300 ºC for 15 min to remove the organic fragments. The process from coating to drying was repeated 10 times before the desired uniform thin films were attained. The same process was repeated for preparing the $FeNiS_2$ doped Leishman stain films [22,23].

Photocatalytic activity: The degradation of three dyes *viz*. methylene blue, malachite green and crystal violet under visible light irradiation, was used to determine the photocatalytic catalytic activity of $FeNiS_2$ doped EDTA and $FeNiS_2$ doped Leishman stain films. In a 100 mL glass tube photochemical reactor, the coated films were placed in a dye solution (methylene blue, malachite green and crystal violet) with a concentration of 10 mg/L for the photocatalytic process. The light source was a low pressure mercury lamp. The cylindrical photoreactor's UV lamp was positioned in its centre and protected by a 25 mm diameter quartz tube. The UV lights and solution surface were separated by no more than 15 cm. The films must then be stored in a dark space to achieve the equilibrium condition (for 30 min). Utilizing a UV-visible spectrophotometer (Agilent Ultraviolet Spectrum carry 8454) with a wavelength of 200-1000 nm, the concentration of each sample was examined [24].

RESULTS AND DISCUSSION

SEM studies: In Fig. 1, in sample $FeNiS_2$ (D1), the iron from the substrate reacted with oxygen from air to form worn scar like structure as a base. However, the sulphur atoms undergo dispersion and moderately decrease from the surface to the interior, which are absolutely survived in the depth of substrate, and nickel presents scattered hexagonal shapes. The $FeNiS_2$ film with EDTA after crystal violet dye degradation (D1CV) also exhibited lightly distorted worn scar texture, which is happened due to the dye degradation. Whereas the $FeNiS_2$ films with EDTA after methylene blue dye (D1MB) and malachite green dye (D1MG) degradation homogeneously covered scatt-

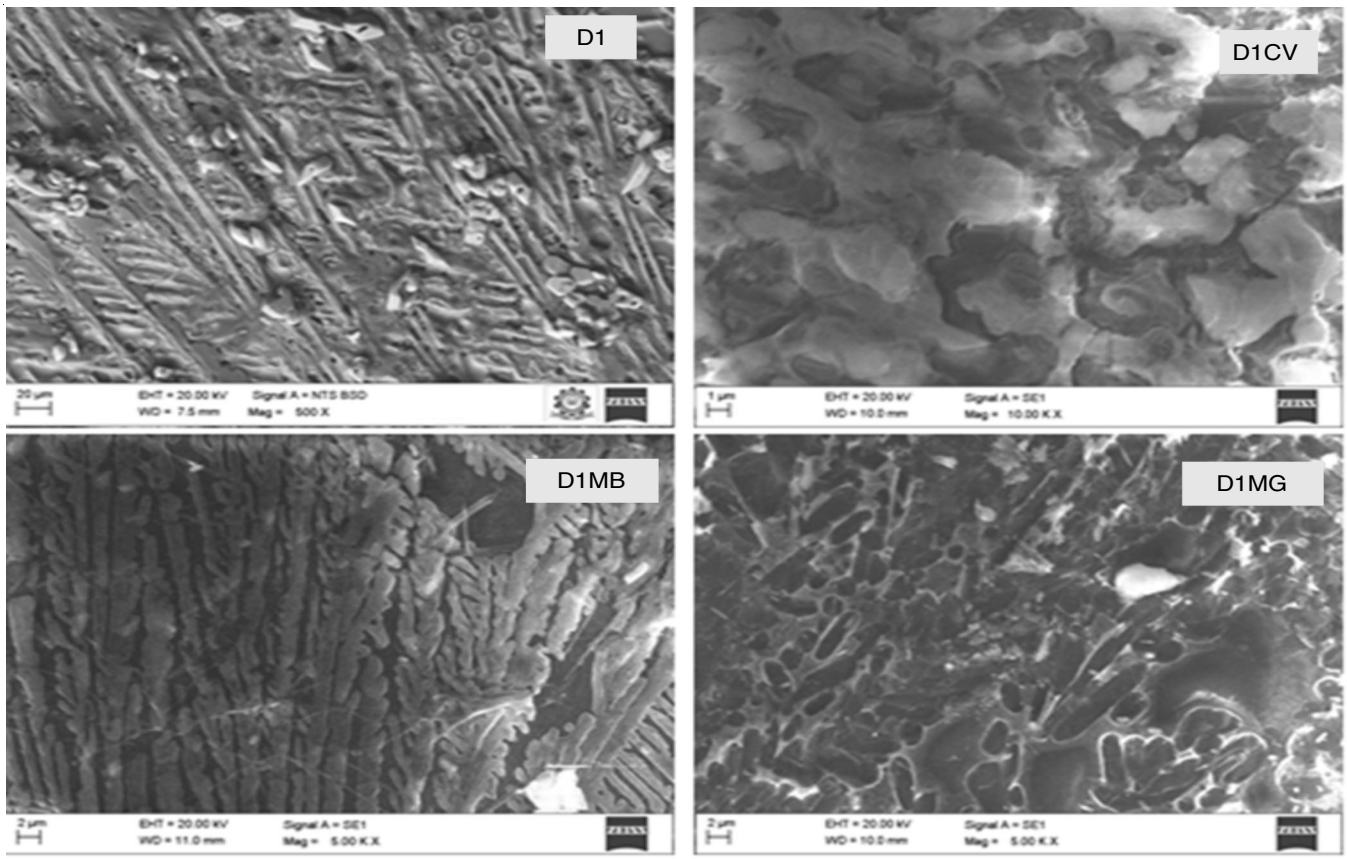

Fig. 1. SEM images of $FeNiS_2$ with EDTA (D1), $FeNiS_2$ with EDTA after degradation of dye crystal violet (D1CV), methylene blue (D1MB) and malachite green (D1MG)

ered crystal growth due to dye degradation. In present studies, the valleys and pinholes of the precursor films in the investigations to date may offer a short channel for atomic diffusion and a sizable surface for the sulfurization reaction.

Similarly in Fig. 2, the $FeNiS_2$ film with Leishman stain, iron as a base, sulphur atoms react with Leishman stain to form some grains and nickel atoms form some partially and fully formed hexagonal shapes. The $FeNiS_2$with Leishman stain after crystal violet dye degradation (D2CV), the morphology depicts the polycrystalline nature of film with random distribution of grains with varying sizes. The $FeNiS_2$ film with Leishman stain after methylene blue dye degradation exhibits porous network like structure (D2MB), whereas $FeNiS_2$ with stain Leishman after malachite green dye degradation (D2MG) depicted that the grain size has irregular agglomeration [25].

EDX studies: The EDAX spectra (Figs. 3 and 4) show the expected elements detected in the prepared thin films. The elemental analysis was carried out only for $FeNiS_2$ with EDTA (D1) the average atomic percentage was found to be 2.4, 1.6, 8.3, 4.5, 6.1, 77.0 for $FeNiS_2$ with EDTA after photocatalytic dye degradation of crystal violet (D1CV) the average atomic percentage was found to be 12.5, 8.7, 57.0, 4.4, 1.3, 8.8, 3.6, 1.1, 1.4, 1.2, $FeNiS_2$ with EDTA after photocatalytic dye degradation of methylene blue (D1MB), the average atomic percentage was found to be 30.9, 1.9, 45.9, 6.1, 1.3, 11.1, 0.4, 1.1, 0.5, 0.1, 0.2, 0.5. The $FeNiS_2$ with EDTA after photocatalytic dye degradation of malachite green (D1MG), the average atomic percentage was found to be 6.8, 6.1, 62.2, 3.4, 1.0, 0.5, 10.7, 3.5, 1.4, 2.7, 2.0.

The $FeNiS_2$ with Leishman stain (D2), the average atomic percentage was found to be 3.4, 2.5, 8.7, 3.5, 2.4, 79.5, $FeNiS_2$ with Leishman stain (D2MG) after photocatalytic degradation of malachite green, the average atomic percentage was found to be 14.2, 3.7, 62.4, 6.3, 0.2, 9.8, 0.7, 0.8, 1.6, 0.3. The $FeNiS_2$ with Leishman stain (D2MB) after photocatalytic dye degradation of methylene blue, the average atomic percentage was found to be 14.8, 3.2, 54.7, 7.9, 1.5, 0.2, 14.7, 0.4, 0.1, 1.4, 0.7, 0.2, whereas the $FeNiS_2$ with Leishman stain (D2CV) after photocatalytic dye degradation of crystal violet the average atomic percentage was found to be 9.1, 1.9, 60.8, 7.2, 1.5, 0.3, 15.2, 0.3, 0.2, 1.5, 1.8 and 0.2. It is thought that these elements may probably results from the microglass slides as a substrate [26].

Mechanism of photocatalytic activity of $FeNiS_2$ doped with EDTA: The mechanism of photo catalytic degradation of dye molecules by $FeNiS_2$ doped with EDTA and Leishman stain thin films are shown below:

$FeNiS_2$ doped with EDTA

$$FeNiS_2C_{10}H_{16}N_2O_8 \rightarrow FeSC_5H_4NO_4(h^+) + NiSC_5H_4NO_4\ (e^-)$$

$$NiSC_5H_4NO_4\ (e^-) + O_2 \rightarrow O_2^{\bullet -}$$

$$O_2^{\bullet -} + H_2O \rightarrow HO_2^{\bullet} + OH^-$$

$$HO_2^{\bullet} + H_2O \rightarrow H_2O_2 + OH^{\bullet}$$

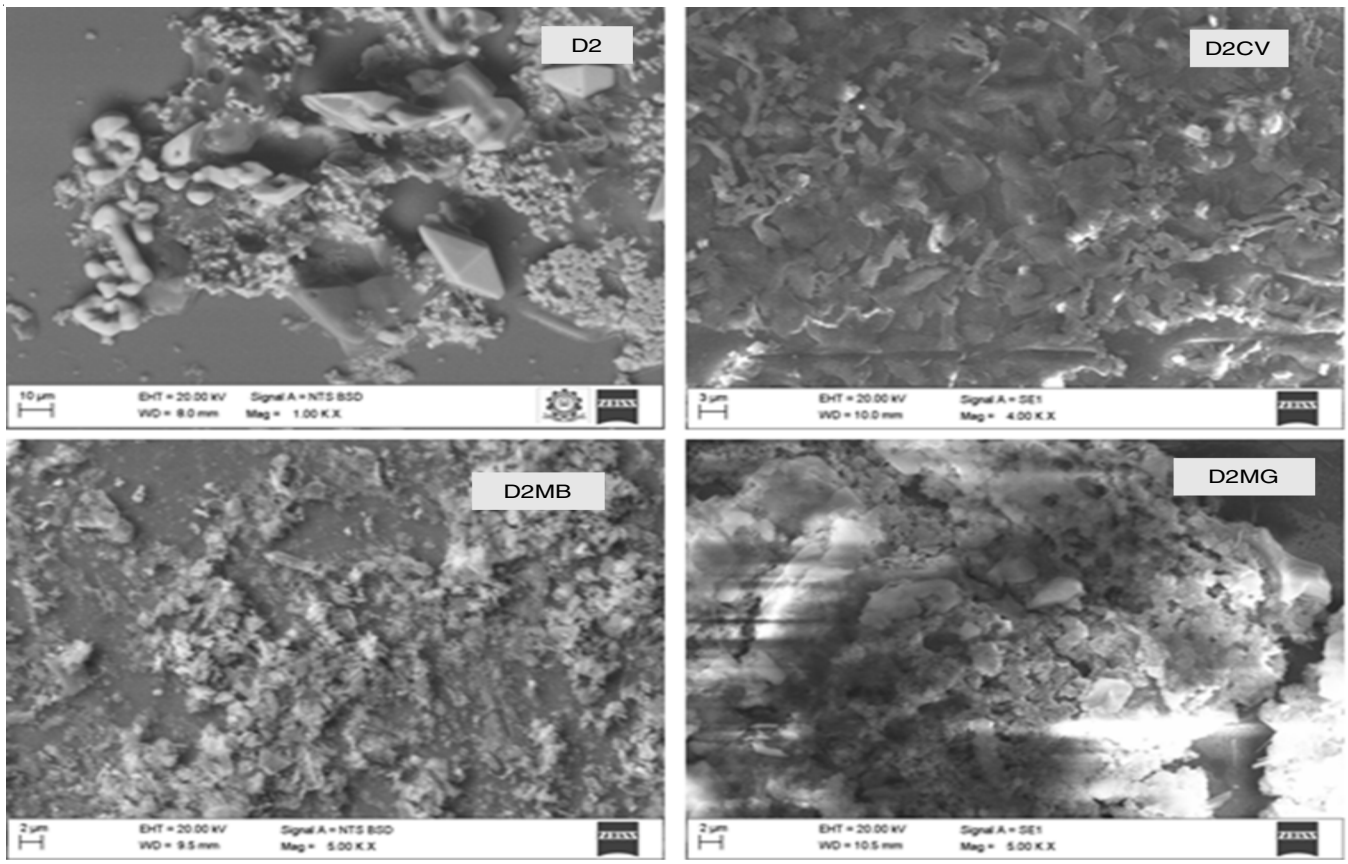

Fig. 2. SEM images of $FeNiS_2$ with Leishman stain (D2), $FeNiS_2$ with Leishman stain after degradation of dye crystal violet (D2CV), methylene blue (D2MB) and malachite green (D2MG)

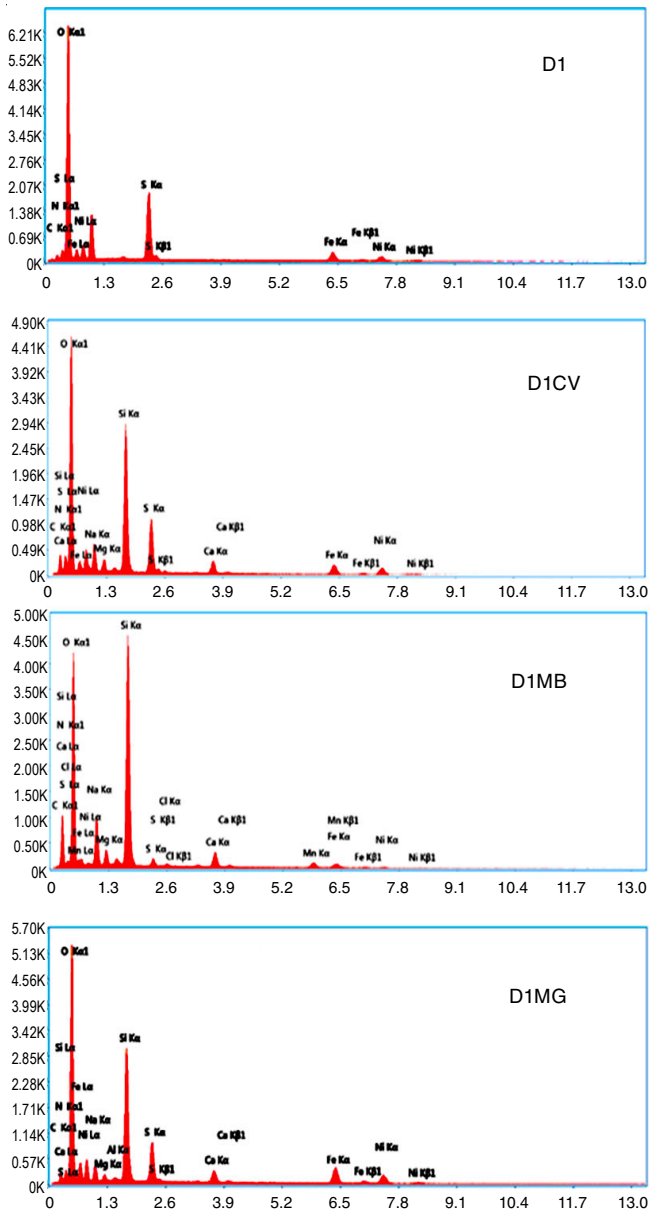

Fig. 3. EDAX analysis of $FeNiS_2$ with EDTA (D1), $FeNiS_2$ with EDTA after degradation of dye crystal violet (D1CV), methylene blue (D1MB) and malachite green (D1MG)

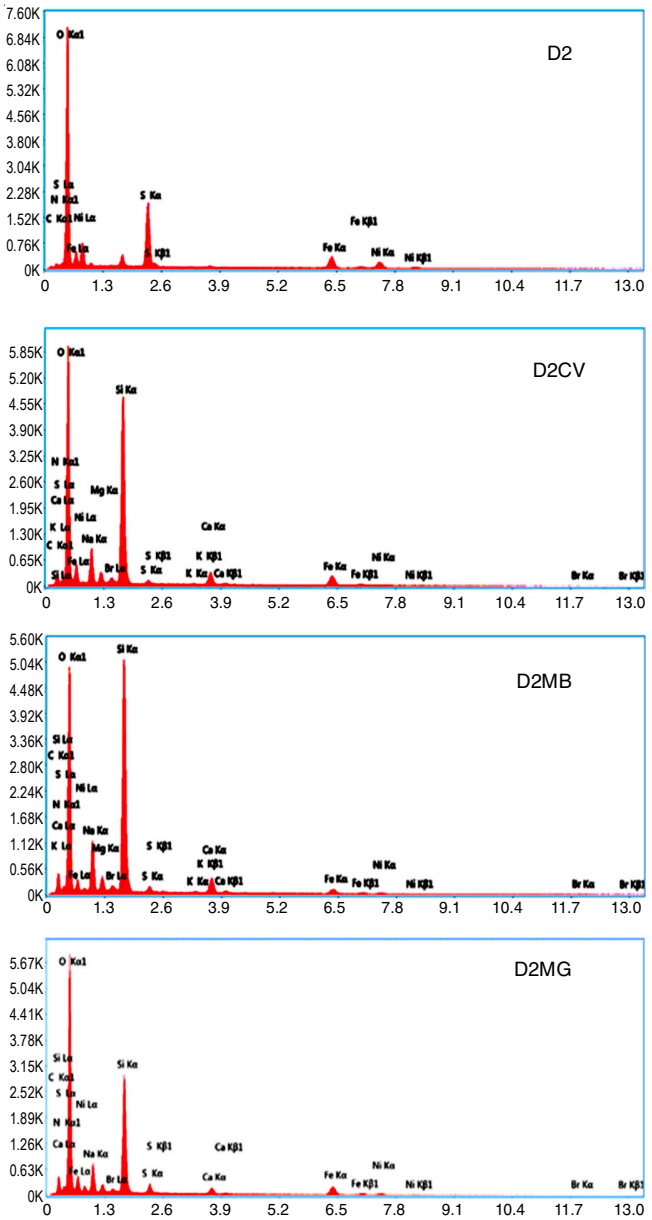

Fig. 4. EDAX spectra of $FeNiS_2$ with Leishman stain (D2), $FeNiS_2$ with Leishman stain after degradation of dye crystal violet (D2CV), methylene blue (D2MB) and malachite green (D2MG)

$$H_2O_2 \rightarrow 2OH^{\bullet}$$

$$FeSC_5H_4NO_4\ (h^+) + H_2O \rightarrow {}^{\bullet}OH$$

$${}^{\bullet}OH + \text{Crystal violet} \rightarrow CO_2 + H_2O$$

$${}^{\bullet}OH + \text{Malachite green} \rightarrow CO_2 + H_2O$$

$${}^{\bullet}OH + \text{Methylene blue} \rightarrow CO_2 + H_2O$$

$FeNiS_2$ doped Leishman stain

$$FeNiS_2C_{16}H_{18}ClN_{35} + C_{20}H_6Br_4Na_2O_5 \rightarrow$$

$$FeSC_{18}H_{12}Br_2ClN_{17}NaO_3(h^+) + NiSC_{18}H_{12}Br_2N_{18}NaO_2(e^-)$$

$$NiSC_{18}H_{12}Br_2N_{18}NaO_2(e^-) + O_2 \rightarrow O_2^{\bullet -}$$

$$O_2^{\bullet -} + H_2O \rightarrow HO_2^{\bullet} + OH^-$$

$$HO_2^{\bullet} + H_2O \rightarrow H_2O_2 + OH^{\bullet}$$

$$H_2O_2 \rightarrow 2OH^{\bullet}$$

$$FeSC_{18}H_{12}Br_2ClN_{17}NaO_3(h^+) + H_2O \rightarrow {}^{\bullet}OH$$

$${}^{\bullet}OH + \text{Crystal violet} \rightarrow CO_2 + H_2O$$

$${}^{\bullet}OH + \text{Malachite green} \rightarrow CO_2 + H_2O$$

$${}^{\bullet}OH + \text{Methylene blue} \rightarrow CO_2 + H_2O$$

Photocatalytic activity of $FeNiS_2$ thin films with different dyes

Degradation of methylene blue: In order to observe the degradation process in terms of colour loss, methylene blue during photocatalytic degradation was recorded at different

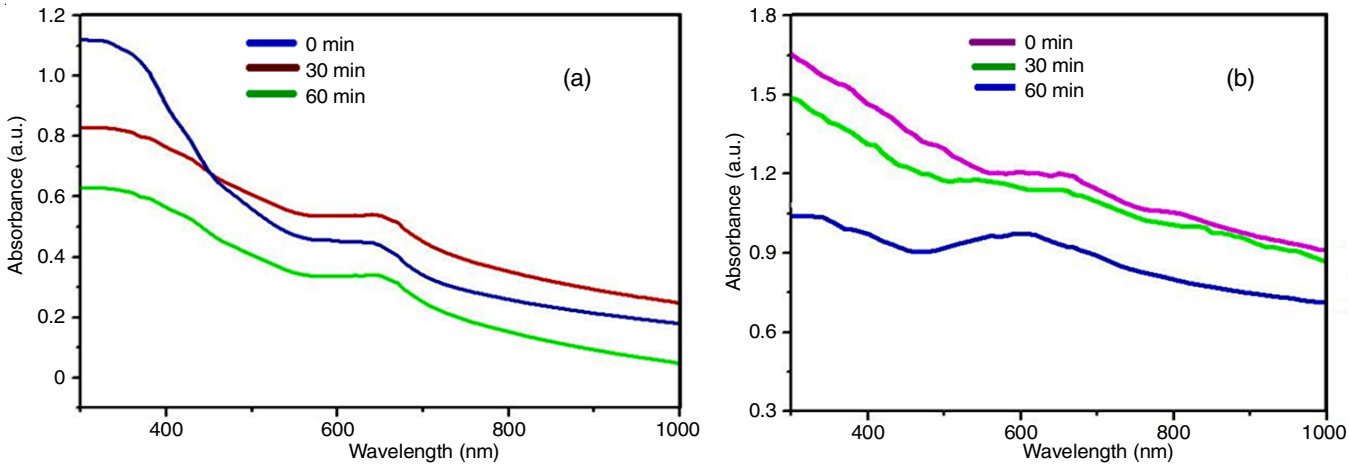

Fig. 5. UV-visible spectra of methylene blue reduction by $FeNiS_2$ with (a) EDTA (D1) and (b) Leishman stain (D2)

time intervals by UV-visible spectrophotometer in 300-1000 nm range. Methylene blue was gradually decomposed and further colour removal due to the additional oxidation-reduction processes, which led to the further degradation of dye molecules into smaller fragments was accomplished over time by the influence of both UV radiation and $FeNiS_2$ photocatalyst, as shown by the continuous decrease in absorbance intensity (Fig. 5). The colour of methylene blue reduced after 60 min of the reaction. Percentage degradation of methylene blue photocatalyzed by $FeNiS_2$ was estimated at different time intervals and the obtained values are calculated [27].

Fig. 6 shows the concentration changes of methylene blue without photocatalyst and over pure $FeNiS_2$ thin films and EDTA, Leishman stain $FeNiS_2$thin films under their radiation of sun light. It is observed that after 60 min, methylene blue degradation ratio is only 7.6% in the absence of catalyst. After 60 min, whereas methylene blue degradation ratio for $FeNiS_2$ thin films was 57%. Methylene blue dye degrades quickly on EDTA and Leishman stain sensitized $FeNiS_2$ thin films utilized as photocatalyst, with 92% methylene blue green degradation ratio after 60 min.

Degradation of crystal violet: Three absorption peaks for crystal violet were observed at wavelengths of 530 nm,

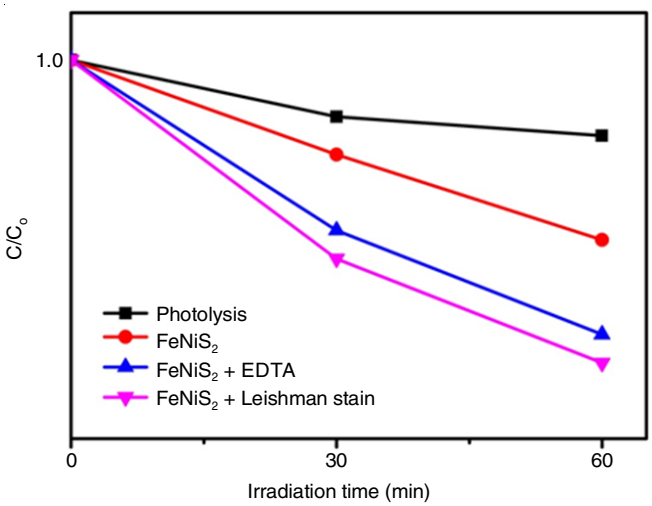

Fig. 6. Photocatalytic degradation of methylene blue using $FeNiS_2$ alone and with EDTA and Leishman stain

510 nm and 500 nm, respectively (Fig. 7). The aromatic ring containing the auxochrome-containing substituent groups (–OH and $-SO_3$) may be responsible for the observed peak in the visible range. The combination of auxochromes and chromo-

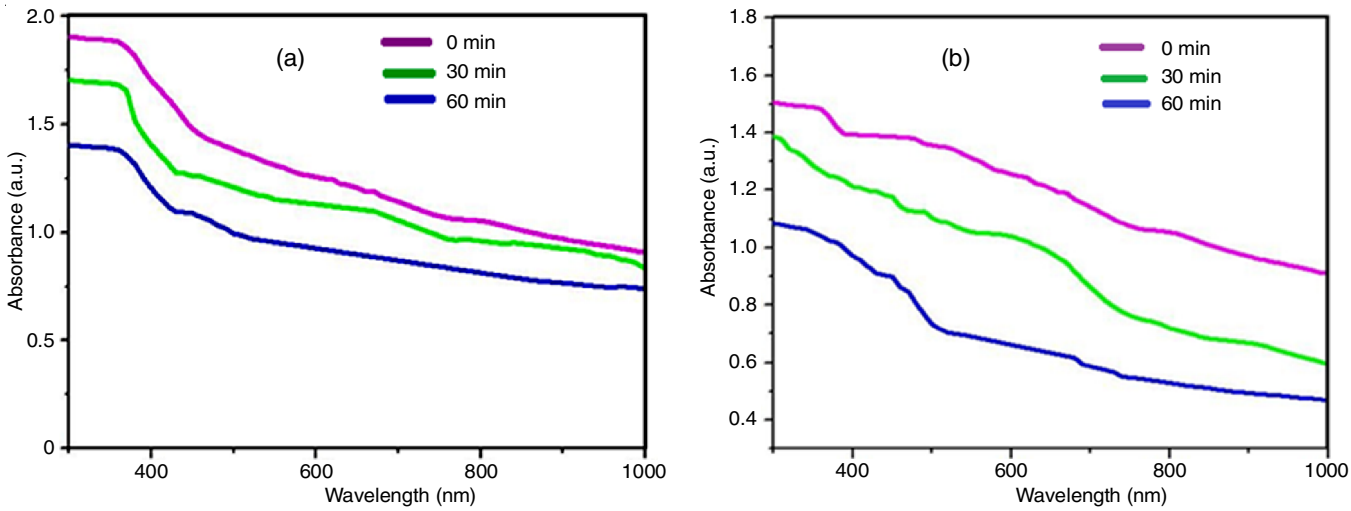

Fig. 7. UV-visible spectra of crystal violet reduction by $FeNiS_2$ with (a) EDTA (D1) and (b) Leishman stain (D2)

phore groups in the crystal violet structure gives the dye its colou and its absorption band intensity increases over time after being exposed to UV radiation with a thin layer of $FeNiS_2$, showing that the chromophoric structure has been destroyed [28].

The concentration variations of crystal violet over pure $FeNiS_2$ thin films, over $FeNiS_2$ thin films with EDTA and over $FeNiS_2$ thin films with Leishman stain are shown in Fig. 8 under the influence of solar radiation. Without a catalyst, the degradation ratio of crystal violet is mere 6.6% after 60 min, however after 60 min, the crystal violet degradation ratio for $FeNiS_2$ thin films is 54%. The reason is attributed due to the rapid deterioration of crystal violet for EDTA and Leishman stain sensitive $FeNiS_2$ thin films employed as photocatalyst, with 90% crystal violet degradation ratio after 60 min [29].

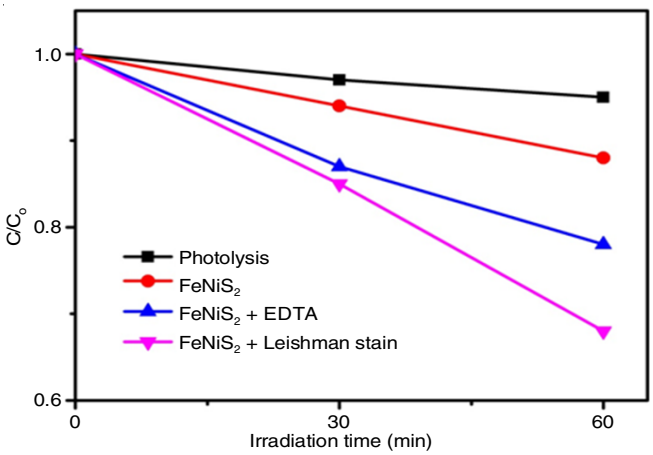

Fig. 8. Photocatalytic degradation of crystal violet using $FeNiS_2$ alone and with EDTA and Leishman stain

Degradation of malachite green: The absorption peak of $FeNiS_2$ catalyst changes towards the longer wavelength range as observed in the UV-vis spectra of $FeNiS_2$ photocatalyst at various time intervals (*e.g.* 0, 30, and 60 min) (Fig. 9). A plot between absorbance and wavelength was used to ascertain the photocatalysts' band gap energies. As exposure time increases, the dye solution's absorbance rises, suggesting that the malachite green dye's concentration has decreased [30].

Malachite green concentration variations are shown in Fig. 10 for three different thin films *viz.* pure $FeNiS_2$ and $FeNiS_2$ thin films with EDTA and Leishman stain, all of which were exposed to sunlight. As can be observed, malachite green degradation after 60 min was only 6.8% without a catalyst. However, after 60 min, 52% malachite green degradation using $FeNiS_2$ thin film was achieved. Moreover, malachite green photocatalyzed degrades quickly using thin $FeNiS_2$ films doped EDTA and Leishman stain with an 89% degradation after 60 min [20]. The degradation efficiency of methylene blue, crystal violet and malachite green dyes after 60 min using $FeNiS_2$, $FeNiS_2$ doped with EDTA and $FeNiS_2$ doped with Leishman stain are shown in Fig. 11.

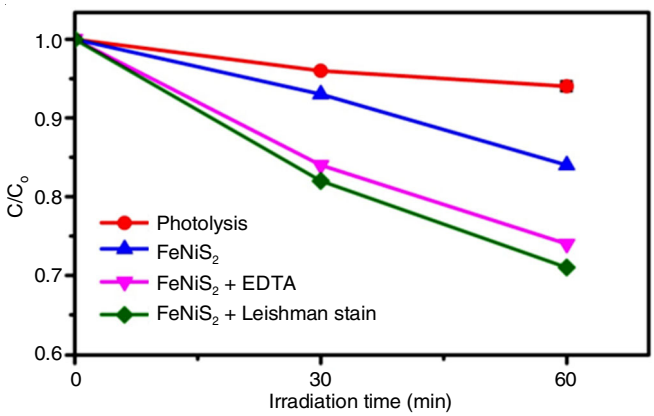

Fig. 10. Photocatalytic degradation of malachite green using $FeNiS_2$ alone and with EDTA and Leishman stain

Conclusion

The $FeNiS_2$ with EDTA and $FeNiS_2$ with Leishman stain thin films were successfully deposited on a glass substrate by sol-gel technique and characterized by SEM and EDX techniques. The photocatalytic behaviour of $FeNiS_2$ with EDTA and $FeNiS_2$ with Leishman stain thin films among methylene blue, crystal violet and malachite green were successfully

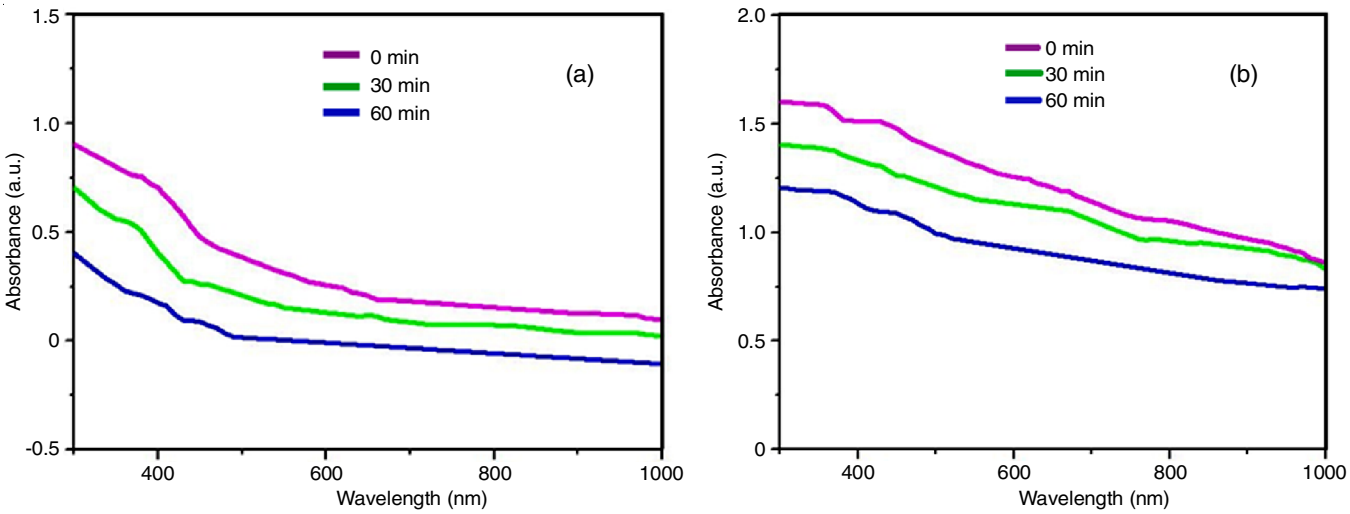

Fig. 9. UV-visible spectra of malachite green reduction by $FeNiS_2$ with (a) EDTA (D1) and (b) Leishman stain (D2)

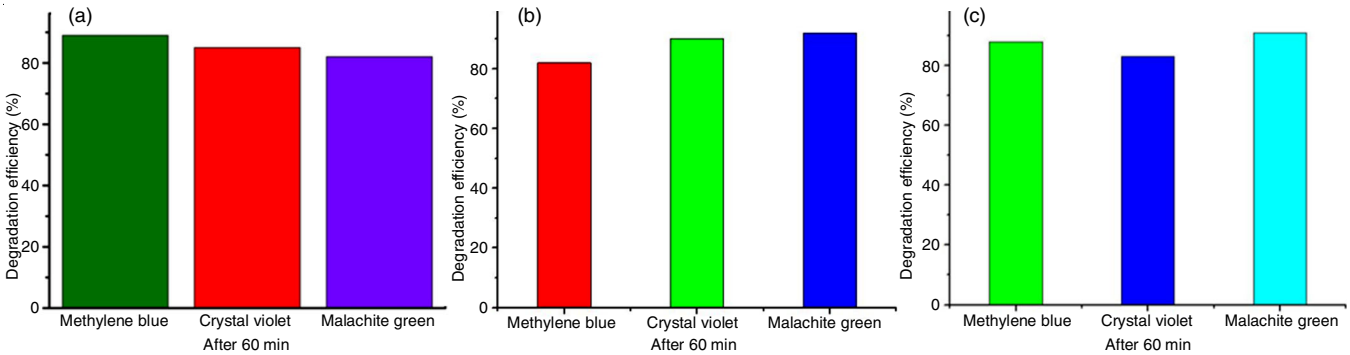

Fig. 11. Degradation efficiency of methylene blue, crystal violet and malachite green using (a) $FeNiS_2$, (b) $FeNiS_2$ with EDTA (D1) and (c) $FeNiS_2$ with Leishman stain (D2)

achieved. Methylene blue, crystal violet and malachite green degradation efficiency were optimum by utilizing $FeNiS_2$ with EDTA and $FeNiS_2$ with Leishman stain thin films on sol-gel method rather than the other tested photocatalysts.

CONFLICT OF INTEREST

The authors declare that there is no conflict of interests regarding the publication of this article.

REFERENCES

1. T.C.M. Santhosh, K.V. Bangeraa and G.K. Shivakumar, *Mater. Sci. Semicond. Process*, **68**, 114 (2017); https://doi.org/10.1016/j.mssp.2017.06.004
2. A.K. Raturi, S. Waita, B. Aduda and T. Nyangonda, *Renew. Ener.*, **11**, 191 (1997); https://doi.org/10.1016/S0960-1481(96)00123-1
3. S. Liu, M. Li, S. Li, H. Li and L. Yan, *Appl. Surf. Sci.*, **268**, 213 (2013); https://doi.org/10.1016/j.apsusc.2012.12.061
4. M. Imran, A. Saleem, N.A. Khan, A.A. Khurram and N. Mehmood, *Thin Solid Films*, **648**, 31 (2018); https://doi.org/10.1016/j.tsf.2018.01.010
5. M.S. Al-Kotb, J.Z. Jumana Al-Waheidi and M.F. Kotkata, *Thin Solid Films*, **631**, 219 (2017); https://doi.org/10.1016/j.tsf.2017.04.017
6. A.C. Berends, M.J.J. Mangnus, C. Xia, F.T. Rabouw and C. de Mello Donega, *J. Phys. Chem. Lett.*, **10**, 1600 (2019); https://doi.org/10.1021/acs.jpclett.8b03653
7. A. Karimi, B. Sohrabi and M.R. Vaezi, *Thin Solid Films*, **651**, 97 (2018); https://doi.org/10.1016/j.tsf.2018.02.021
8. J. Puthussery, S. Seefeld, N. Berry, M. Gibbs and M. Law, *J. Am. Chem. Soc.*, **133**, 716 (2011); https://doi.org/10.1021/ja1096368
9. V. Kumar, J.K. Singh and G.M. Prasad, *Indian J. Pure Appl. Phys.*, **53**, 429 (2015).
10. U. Syafiq, E. Isotta, N. Ataollahi, K. Lohani, S. Luong, V. Trifiletti, O. Fenwick and P. Scardi, *ACS Appl. Energy Mater.*, **5**, 5909 (2022); https://doi.org/10.1021/acsaem.2c00268
11. J. Woon-Jo and P. Cye-Choon, *Sol. Energy Mater. Sol. Cells*, **75**, 93 (2003); https://doi.org/10.1016/S0927-0248(02)00110-1
12. S.C. Ezugwu, F.I. Ezema and P.U. Asogwa, *Chalcogenide Lett.*, **7**, 341 (2010).
13. D.M. Berg, R. Djemour, L. Gütay, G. Zoppi, S. Siebentritt and P.J. Dale, *Thin Solid Films*, **520**, 6291 (2012); https://doi.org/10.1016/j.tsf.2012.05.085
14. S.H. Pawar, S.P. Tamhankar, C.D. Lokhande, *Sol. Energy Mater.*, **14**, 71 (1986); https://doi.org/10.1016/0165-1633(86)90014-6
15. J.-H. Lee, W.-C. Song, J.-S. Yi and Y.-S. Yoo, *Sol. Energy Mater. Sol. Cells*, **75**, 227 (2003); https://doi.org/10.1016/S0927-0248(02)00164-2
16. K. Nair and M.T.S. Nair, *Semicond. Sci. Technol.*, **7**, 239 (1992); https://doi.org/10.1088/0268-1242/7/2/011
17. A. Cruz-Vazquez, F. Rocha-Alonzo, S.E. Burruel-Ibarra, M. Inoue and R. Bernal, *Superficies y Vacio*, **13**, 89 (2001).
18. G. Murtaza, S. Alderhami, Y.T. Alharbi, U. Zulfiqar, M. Hossin, A.M. Alanazi, L. Almanqur, E.U. Onche, S.P. Venkateswaran and D.J. Lewis, *ACS Appl. Energy Mater.*, **3**, 1952 (2020); https://doi.org/10.1021/acsaem.9b02359
19. E. Anuja, K. Manikandan and R. Thiruneelakandan, *J. Mater. Sci.: Mater. Electr.*, **29**, 9886 (2018); https://doi.org/10.1007/s10854-018-9030-3
20. G.D. Gayathri, K. Manikandan and R. Thiruneelakandan, *J. Mater. Sci.: Mater. Electr.*, **30**, 6023 (2019); https://doi.org/10.1007/s10854-019-00903-2
21. E. Sindhuja, K. Ravichandran and K. Shanthaseelan, *Mater. Res. Bull.*, **103**, 299 (2018); https://doi.org/10.1016/j.materresbull.2018.03.007
22. T. Ivanova, A. Harizanova, T. Koutzarova and B. Vertruyen, *Mater. Lett.*, **64**, 1147 (2010); https://doi.org/10.1016/j.matlet.2010.02.033
23. P. Trilok Kumar, K.P. Pankaj, G. Himanshu, M. Gagan, K. Ajendra, R. Kumar and L.P. Purohit, *J. Environ. Rehab. Conserv.*, **6**, 184 (2015).
24. L. Ren, Y. Li, J. Hou, X. Zhao and C. Pan, *ACS Appl. Mater. Interfaces*, **6**, 1608 (2014); https://doi.org/10.1021/am404457u
25. P.C. Huang, W.C. Yang and M.W. Lee, *J. Phys. Chem.*, **C117**, 18308 (2013); https://doi.org/10.1021/jp4046337
26. B. Guzeldir, M. Saglam and A. Ates, *Acta Phys. Polon. A*, **121**, 33 (2011).
27. A.O. Ibhadon and P. Fitzpatrick, *Catalysts*, **3**, 189 (2013); https://doi.org/10.3390/catal3010189
28. M. Umehara, Y. Takeda, T. Motohiro, T. Sakai, H. Awano and R. Maekawa, *Appl. Physics Express*, **6**, 045501 (2013); https://doi.org/10.7567/APEX.6.045501
29. K. Ravichandran and E. Sindhuja, *Mater. Chem. Phys.*, **221**, 203 (2019); https://doi.org/10.1016/j.matchemphys.2018.09.038
30. N.L. Becerril-Altamirano, R.T. Hernández López, L. González-Reyes A.R. Suárez-Parr, R. Ramírez-López, A. Martínez-Jiménez and I. Hernández-Pérez, *J. Phys.: Conf. Ser.*, **1221**, 012027 (2019); https://doi.org/10.1088/1742-6596/1221/1/012027